Point mutated Caveolin-3 form (P104L) impairs myoblast differentiation via Akt and p38 signalling reduction, leading to an immature cell signature

Point mutated Caveolin-3 form (P104L) impairs myoblast differentiation via Akt and p38 signalling reduction, leading to an immature cell signature

Elena Stoppani [1], Stefania Rossi [1], Elisabetta Meacci [2], Fabio Penna [3], Paola Costelli [3], Arianna Bellucci [1], Fiorella Faggi [1], Daniele Maiolo [1], Eugenio Monti [1], Alessandro Fanzani [1*]

Addresses

[1] Department of Biomedical Sciences and Biotechnologies, University of Brescia, Italy.

[2] Department of Biochemical Sciences, University of Florence, Italy.

[3] Department of Experimental Medicine and Oncology, University of Turin, Italy.

[*] *Corresponding author*. Fax +39 030 3701157

E-mail address: fanzani@med.unibs.it (Alessandro Fanzani)

The abbreviations used are: bHLH, basic helix-loop-helix; BSA, bovine serum albumin; CMV, cytomegalovirus; DMEM, Dulbecco's modified Eagle's Medium; FBS, foetal bovine serum; GAPDH, glyceraldehyde 3-phosphate dehydrogenase; HS, horse serum; IGF-1, Insulin-like growth factor-1; MAPK, mitogen-activated protein kinases; MCK, muscle creatine kinase; MLC, myosin light chain; MMLV-RT, Moloney Murine Leukemia Virus Reverse Transcriptase; MyHC, myosin heavy chain; PBS, phosphate buffer solution; PI3K, phosphatydil-inositol-3-kinase; TGF-β, Transforming Growth Factors beta.

Keywords: Caveolin-3; skeletal myoblasts; Akt; p38 MAPK; TGF-β.

Abstract

Unbalanced levels of Caveolin-3 (Cav3) are involved in muscular disorders. In the present study we show that differentiation of immortalized myoblasts is affected by either lack or over-expression of Cav3. Nevertheless, depletion of Cav3 induced by delivery of the dominant-negative Cav3 (P104L) form elicited a more severe phenotype, characterized by the simultaneous attenuation of the Akt and p38 signalling network, leading to an immature cell and molecular signature. Accordingly, differentiation of myoblasts harbouring Cav3 (P104L) was improved by countering the reduced Akt and p38 signalling network via administration of IGF-1 or Trichostatin A. Furthermore, loss of Cav3 correlated with a deregulation of the TGF-β-induced Smad2 and Erk1/2 pathways, confirming that Cav3 controls TGF-β signalling at the plasma membrane. Overall, these data suggest that loss of Cav3, primarily causing attenuation of both Akt and p38 pathways, contributes to impair myoblast fusion.

Introduction

Caveolae and caveolins play a prominent role to regulate signal transduction [1-3]. Caveolin-3 (Cav3) is preponderantly expressed in the skeletal muscle, contributing to proper differentiation of myoblasts and homeostasis of myofibers [4-6]. Through its scaffolding domain, Cav3 interacts with different proteins at the plasma membrane, thereby influencing their biological activity, as occurs for the nitric oxide synthase [7-9], Src tyrosine kinase [10,11], Alk4 and 5 receptors [12] and PI3K-Akt kinases [13-15]. Cav3 expression must be tightly regulated, as demonstrated by the fact that either a deficiency or an excess cause muscular disorders. In particular, loss of Cav3 at the sarcolemma is a feature sign of caveolinopathies, an heterogeneous group of genetic diseases caused by Cav3 mutations giving rise to dominant-negative protein forms [16-20]. The missense Cav3 (P104L) substitution is frequently associated to the human Limb Girdle Muscular Dystrophy 1-C (LGMD1C, OMIM #607801) [16], and its transgenic delivery causes muscular defects also in mice and zebrafish models [9,12,21]. In addition, even an excess of Cav3 causes of a Duchenne-like muscular phenotype in transgenic mice [22], definitely suggesting that Cav3 levels influence the muscle homeostasis. In the present study we employed immortalized murine myoblasts to analyse the effects of either Cav3 (P104L) or wild-type Cav3 delivery on cell fusion, a process that is crucial during embryonal differentiation or muscle regeneration. We found that both low and high Cav3 levels affect myoblast fusion. In particular, a more severe phenotype was conferred by the loss of Cav3, basically correlating with the attenuation of Akt and p38 activities but also with the perturbation of TGF-β signalling. In addition, we show that differentiation of myoblasts harbouring the Cav3 (P104L) form was improved by the administration of IGF-1 or Trichostatin A, two molecules promoting muscle hypertrophy [23,24].

Materials and methods

Materials

All the reagents were from Sigma-Aldrich, unless differently indicated.

Cell cultures and morphometric analysis of myotubes

Mouse C2C12 and rat L6E9 myoblasts were maintained under standard conditions (37°C and 5% CO_2 in humidified incubator) and cultured in a high-serum medium, consisting of high-glucose DMEM supplemented with 10% or 20% FBS, respectively, in the presence of 100 μg/ml penicillin-streptomycin antibiotic. To induce differentiation, 80% confluent C2C12 or L6E9 myoblasts were switched to a low-serum medium (termed differentiating medium, DM), consisting of DMEM supplemented with 2% HS or 1% FBS, respectively. To visualize myotubular structures, cells were fixed in methanol and stained with Giemsa reactive. An Image ProPlus software (version 6.2) was used to quantify the size of myotubes. The average size was calculated as the mean of 100 samples, as obtained by measuring 10 myotubes in 10 different fields.

Plasmids and cell transfections

The plasmids harbouring either the wild-type Cav3 or the Cav3 (P104L) form, under the control of a CMV promoter (pCAGGS vectors), were kindly provided by Ferruccio Galbiati (University of Pittsburgh, USA). To allow post-mitotic expression of mutant, Cav-3 (P104L) cDNA was excised by pCAGGS vector with EcoRI restriction enzyme (Promega) and ligated into a pGEX-KG plasmid; then cDNA was excised again by double digestion with SmaI and SacI (Promega), and eventually ligated into the pMEX vector containing a MLC promoter [25]. Transfections were carried out by using Lipofectamine 2000 reagent (Invitrogen), according to manufacturer's instructions. To isolate antibiotic-resistant clones, C2C12 and L6E9 were cotransfected with pcDNA or pBabe vectors, and cultured in high-serum medium supplemented with geneticin (0.5 mg/ml) or puromycin (1 μg/ml), respectively.

Drug treatments

The pharmacological SB203580 compound (5 μM) was used to inhibit p38 activity, whereas LY294002 (5 μM, a PI3K inhibitor) was used to block Akt activity. To induce myotube hypertrophy, IGF-1 (50 ng/ml) was administered to myoblasts after 2 days of differentiation, in order to avoid hyper-proliferative effects [23]. Alternatively, myoblasts were treated with Trichostatin A (TSA), an inhibitor of histone deacetylases, which raises the endogenous expression of follistatin and enhances the size of myotubes [24]. In particular, TSA (50 nM) was administered to 80% confluent cells for up to 16-18 hours before addition of DM. Human recombinant TGF-β (Peprotech) was administered to myoblasts at the dose of 5 ng/ml.

RNA isolation and semi-quantitative RT-PCR analysis

Total RNA was isolated by Tri-reagent method and digested with DNAse (DNA-free, Ambion). RNA (2 μg) was reverse-transcribed in presence of 400 units of MMLV-RT (Promega) and the template was used for PCR amplification. The following forward (F) and reverse (R) primers (250 nM each) were used:

Gene	Primers	Sequence	PCR Cycles	Size
Cav3	F R	ACCCCAAGAACATCAATGAG TGCAGAAGGTGCGGATACAC	26	310 bp
MyoD	F R	CTGCTCTGATGGCATGATGGATTAC AGAGCACCTGGTAAATCGGATTGG	28	343 bp
Myf-5	F R	AGCCCACCAGCCCCACCTC TTCTGCCCAGCTTTTCTTTCCTTC	30	394 bp
Myogenin	F R	CCAGGAGCCCCACTTCTATGACGGGG TGATGCTGTCCACGATGGACGTAAGGG	24	590 bp
Follistatin	F R	CTCTTCAAGTGGATGATTTTC ACAGTAGGCATTATTGGTCTG	30	334 bp
GAPDH	F R	GGTGCTGAGTATGTCGTGGAGTC GGACTGTGGTCATGAGCCCTTCC	21	267 bp

Luciferase assays

Gene reporter assays were carried out by using the Promega Dual Luciferase assay system, according to manufacturer's instructions. Cells were transiently transfected with vectors harbouring

the reporter gene under the control of a MCK promoter or a four MyoD responsive element (4RE) [26,27], in combination with the pRL-TK-Renilla luciferase control vector to correct the transfection efficiency.

Antibodies

The following primary monoclonal antibodies were used: mouse anti-Cav3 (clone 26, BD Transduction Laboratories), mouse anti-GM130 (BD Transduction Laboratories), rabbit anti-MyoD (clone M-318, Santa Cruz Biotechnology), mouse anti-Myf5 (clone C-20, Santa Cruz Biotechnology), mouse anti-myogenin (clone F5D, Santa Cruz Biotechnology), mouse anti-MyHC (Hybridoma Bank, University of Iowa), rabbit anti-cyclin D1 (clone H295, Santa Cruz Biotechnology), and mouse anti-alpha-tubulin (clone B-5-1-2, Sigma-Aldrich). Rabbit polyclonal antibodies from Cell Signaling were used to detect the phosphorylated Akt (Ser^{473}) and p38 (Thr^{180}/Tyr^{182}) and total forms. Phosphorylated (Tyr^{204}) and total Erk1/2 forms were recognized by using mouse monoclonal antibodies from Santa Cruz Biotechnology.

Western-blot analysis

Protein concentration was calculated by bicinchoninic acid assay (Pierce). Equal amounts of protein samples were separated by SDS-PAGE under reducing conditions and transferred to PVDF membranes. Incubation with specific primary antibodies was followed by horseradish peroxidase-conjugated secondary antibodies (Chemicon), and the immunocomplexes were visualized using enhanced chemiluminescence reagent (Chemicon, Cat. number 2600-5). To analyse cyclin D1, MyoD, Myf-5, myogenin and MyHC, myoblasts were harvested in a cold RIPA lysis buffer, composed by 20 mM Tris-HCl (pH 7.6), 1% Nonidet P40, 0.5% sodium deoxycholate, 0.1% SDS, 50 mM NaCl, and a mix of proteases inhibitors (Roche Molecular Biochemicals). To analyse Cav3 expression, myoblasts were harvested in a cold Triton lysis buffer, composed by 10 mM Tris-HCl (pH 8.0), 1% Triton X-100, 5 mM EDTA, 150 mM NaCl and a mix of proteases inhibitors. Then cell lysates were centrifuged (12,000 x g for 15 min at 4°C) and the Triton-insoluble cell membranous fractions were used for Cav3 analysis. To analyse phosphorylated and total Akt, p38

and Erk1/2 forms, myoblasts were harvested in a cold lysis buffer composed by 20 mM Tris-HCl (pH 7.4), 0.2% Triton X-100, 1 mM EDTA, 150 mM NaCl, and a mix of proteases and phosphatases inhibitors (0.5 mM NaF and Na_3VO_4).

Immunofluorescence microscopy

C2C12 myoblasts were cultured on 12 mm glass coverslips coated with 20 μg/ml laminin (Roche). Then cells were fixed with paraformaldehyde for 10 min at 37°C, washed with PBS/sucrose (2%) and treated with an extraction buffer, composed by 20 mM Hepes (pH 7.4), 0.5% Triton X-100, 300 mM sucrose, 3 mM $MgCl_2$ and 50 mM NaCl. Subsequently, C2C12 were treated with 3% BSA in PBS for 15 min, and incubated for 2 hours in a humid atmosphere in the presence of a diluted anti-Cav3 antibody (1:800), anti-GM130 antibody (1:500), or anti-MyHC antibody (1:200). After PBS washing, samples were incubated for 1 hour in the presence of a diluted anti-mouse or anti-rabbit CY3 conjugated secondary antibody (1:1000, Jackson Immunoresearch). Cells were visualized by means of a Zeiss confocal microscope (Carl Zeiss S.p.A.), with the laser set on λ = 405-488-543 nm and the height of the scanning = 1 μm. Images (512 x 512 pixels) were then reconstructed using LSM Image Examiner software (Carl Zeiss S.p.A.). Alternatively, fluorescent staining was observed under an Axiovert S100 microscope (Zeiss), and pictures were taken with a digital camera (SensiCam) using the Image-Pro Plus software (version 6.2).

Statistics

All of the data are expressed as means ± S.E. Statistical significance was determined using *t*-Student analysis. A p value of <0.05 was considered significant.

Results

Cell fusion of immortalized myoblasts is more severely affected by loss rather than excess of Cav3.

Transgenic mice harbouring inactivating Cav3 (P104L) mutation display loss of Cav3 at the plasmalemma and a severe muscle atrophy [9,12], whereas mice over-expressing wild-type Cav3 form (wtCav3) undergo a Duchenne-like muscular phenotype [22], suggesting that proper levels of Cav3 are crucial for maintaining the muscle homeostasis. In keeping with these observations, we stably over-expressed either mutated or wtCav3 form in C2C12 myoblasts to analyse the effects on the differentiation process. Compared to control cells delivered with an empty vector, transgene expression produced a significant increase of both Cav3 transcripts (Fig. 1A). However, whereas transfection of wild-type form produced Cav3 protein accumulation, Cav3 (P104L) triggered a substantial loss of Cav3 (Fig. 1A). This is consistent with previous observations indicating that mutated Cav3 proteins display reduced protein half-life and behave with a dominant-negative fashion, aggregating with the wild-type forms within the Golgi apparatus, eventually causing loss of Cav3 at the plasma membrane [19,20]. Confocal microscopy analysis showed that an antibody for Cav3 marked perinuclear regions in Cav3 (P104L) myoblasts, which were positively co-stained with antibodies for GM130 [28], a typical Golgi marker (Fig. 1B). On the other side, Cav3 labelling was predominantly localized at the plasma membrane in wtCav3 over-expressing cells, although the staining displayed a stronger intensity compared to control myotubes (Fig. 1B). Both of these conditions (low Cav3 vs. high Cav3 at the plasma membrane) impaired C2C12 myoblasts differentiation, but besides them, the presence of Cav3 (P104L) induced a more severe phenotype, as determined by the analysis of MyHC expression (Fig. 1A) and the evaluation of morphological differentiation (Fig. 1B). In particular, the formation of myotubes was almost abolished in the presence of Cav3 (P104L) form (Fig. 1B and graphical panel), likely suggesting that loss of Cav3, more potently than overexpression, inhibits myoblast fusion. Since Cav3 expression is physiologically restricted to myoblasts undergoing differentiation and mature myofibers [4,5], we

generated a vector harbouring Cav3 (P104L) under the control of a post-mitotic MLC promoter. Expression of MLC-Cav3 (P104L) impaired the myoblast fusion in both immortalized C2C12 and L6E9 cell lines compared to control (Fig. 2A), despite less severely in comparison with CMV-Cav3 (P104L), as evidenced by the presence of thin myotubes (Fig. 2A,B) and a residual MyHC expression (Fig. 2C). Taken together, these data provide evidence that loss of Cav3 at the plasma membrane, as induced by Cav3 (P104L) expression, severely delays the myoblast fusion.

Cav3 (P104L) imposes an immature molecular signature, dependent on the attenuation of Akt and p38 signalling network.

We investigated the molecular mechanisms underlying the defective cell fusion in myoblasts harbouring Cav3 (P104L) form under the control of MLC promoter. To this purpose, we first looked at the Akt and p38 pathways, as this signalling network is pivotally involved in the proper coordination of myogenic commitment [29]. Throughout a time-course differentiation, Western-blot analyses detected that the loss of Cav3 induced by mutant expression correlated with the decreased levels of phosphorylated Akt and p38 forms compared to control cells (Fig. 3A), leading to an altered expression pattern of the bHLH transcription factors, such as MyoD, Myf-5 and myogenin [30,31]. In particular, loss of Cav3 conferred a molecular signature reminiscent of an immature cell state [32], being characterized by the decreased levels of MyoD and myogenin and increased levels of Myf-5 compared to control, as further corroborated by RT-PCR analysis (Fig. 3B). As confirmed by the luciferase reporter assays, the ability of MyoD to transactivate a MCK promoter or a minimal 4RE element [26,27] was effectively impaired in MLC-Cav3 (P104L) cells compared to control (Fig. 3C). In addition, MLC-Cav3 (P104L) myoblasts also displayed a premature cyclin D1 disappearance compared to control (Fig. 3A), an event normally preluding to myogenic commitment [33], but which can also be a consequence of the PI3K/Akt pathway down-regulation [34,35]. Unlikely observed in the absence of Cav3, the phosphorylation of Akt and p38 kinases was not decreased by wtCav3 over-expression (Fig. 3D), suggesting that lack or excess of Cav3 affect myoblast fusion through different mechanisms. Subsequently, we aimed to establish whether the

pharmacological inhibition of p38 and Akt activities, as obtained by respectively administering SB203580 (SB) or LY294002 (LY) compounds, was sufficient to reproduce in control myoblasts the molecular pattern recognized in MLC-Cav3 (P104L) myoblasts. Inhibition of either pathway was sufficient to preclude differentiation (not shown), leading to down-regulation of MyoD compared to DMSO-treated cells (Fig. 4A). In the presence of SB, however, cyclin D1 remained elevated, being the activity of p38 required for the proper cell cycle exit [36], further contributing to maintain elevated Myf-5 levels in comparison with DMSO (Fig. 4A). In the presence of LY, on the contrary, both Myf-5 and cyclin D1 were down-regulated compared to DMSO (Fig. 4A), confirming that the sole inhibition of either pathway affects differentiation but leading to a different molecular signature. Remarkably, the simultaneous administration of both SB and LY inhibitors impaired differentiation of C2C12 myoblasts (Fig. 4B) and decreased the protein content of MyoD, cyclin D1 and myogenin, leading to sustained Myf-5 levels (Fig. 4C), thus eliciting the molecular signs observed in MLC-Cav3 (P104L) myoblasts. Accordingly, 4RE reporter activity was prevented in C2C12 myoblasts treated with SB and LY compared to DMSO, as assayed after a transient transfection for up to 24 hours (Fig. 4D). Overall, these results indicate that, in our established *in vitro* models, loss of Cav3 imposes a particular immature cell and molecular signature largely reminiscent of the simultaneous down-modulation of Akt and p38 signalling network.

Lack of Cav3 perturbs the activation of TGF-β pathways.

It has been shown that, at the plasma membrane, Cav3 physically interacts with type I TGF-β receptors (termed Alk4 and Alk5) to limit the activity of Smad2 pathway [12]. For this reason, atrophic muscles of transgenic Cav3 (P104L) mice exhibit increased Smad2 signalling [12]. TGF-β superfamily members, such as TGF-β or myostatin, bind different specific type II TGF-β receptors but commonly employ Alk4 or 5 receptors to activate Smad-dependent and -independent pathways, including Smad2, Smad 3 and Erk1/2 [37,38]. Activation of TGF-β pathways exerts an inhibitory effect on the myoblast differentiation, causing down-regulation of the Akt pathway [39,40], loss of cyclin D1 [34,35], MyoD [41] and myogenin [42], which are all hallmark signs recognized in MLC-

Cav3 (P104L) myoblasts. Thus, we investigated whether an involvement of the TGF-β pathways might account for the cell behaviour observed upon Cav3 loss. After 2 days of differentiation, the basal levels of Erk1/2 phosphorylation appeared slightly but significantly reduced in MLC- and CMV-Cav3 (P104L) myoblasts compared to control, whereas Smad2 and 3 phosphorylation levels were unchanged (Fig. 5). Administration of TGF-β rapidly induced the phosphorylation of Smad2, Smad3 and Erk1/2 in control, while eliciting a stronger phosphorylation of Smad2, but not Smad3, in Cav3 (P104L) myoblasts, thus conforming previous *in vivo* findings [9]. Consistently, the TGF-β-induced Erk1/2 phosphorylation was diminished in Cav3 (P104L) myoblasts compared to control (Fig. 5). Taken together, these data indicate that loss of Cav3 predisposes to over-activation of Smad2 together with down-regulation of Erk1/2 pathways exclusively in the presence of TGF-β trigger. In addition, these data indirectly suggest that the attenuation of Akt and p38 signalling observed in Cav3 (P104L) myotubes likely occurs independently on the activation of TGF-β pathway.

Stimulation of the Akt and p38 signalling network, via administration of IGF-1 or Trichostatin A, improves the differentiation of myoblasts even in absence of Cav3.

We asked whether administration of molecules normally promoting myotubes hypertrophy might improve the differentiation of Cav3 (P104L) myoblasts. In particular, we employed IGF-1, a growth factor exerting an anabolic effect on the skeletal myofibers [23], or Trichostatin A (TSA), an inhibitor of histone deacetylases which promotes increased cell fusion by raising the expression of follistatin [24]. Phase contrast pictures and immunofluorescent MyHC staining indicated that the treatments effectively improved the differentiation of MLC-Cav3 (P104L) myoblasts, with a more pronounced effect in the case of TSA treatment (Fig. 6A). Both the treatments did not significantly affect the number of MyHC positive ($MyHC^{+}$) myotubes (Fig. 6B), rather their size (Fig. 6C). In MLC-Cav3 (P104L) myoblasts treated with IGF-1 or TSA, Cav3 clearly remained mislocalized to the Golgi apparatus and a recovery at the plasma membrane was not observed (Fig. 6A). Interestingly, exposure of MLC-Cav3 (P104L) myoblasts to TSA, followed by post-mitotic IGF-1

treatment, elicited the formation of giant myotubes, featured by an intense perinuclear Cav3 staining (Fig. 6D), thus confirming the ability of these cells to increase their size regardless of the improper Cav3 localization. As evaluated at transcript levels, TSA was effectively able to raise follistatin expression in both MLC-Cav3 (P104L) myoblasts and control cells (Fig. 7A) [24]. In the presence of IGF-1 or TSA, Western-blot analyses showed that the phosphorylation of both Akt and p38 kinases was partially re-enabled in MLC-Cav3 (P104L) myoblasts (Fig. 7B). Thus, the treatments produced a rescue of MyoD and myogenin levels and elicited a gradual Myf-5 disappearing in MLC-Cav3 (P104L) myoblasts (Fig. 7D), leading to a recovery of MyHC during the differentiation (Fig. 7E). Taken together, these results indicate that both IGF-1 and the histone deacetylase inhibitor TSA are effective to enhance differentiation in myoblasts harbouring Cav3 (P104L) form.

Discussion

Cav3 represents a first-line checkpoint for the regulation of cell signalling in muscle cells [1-3]. By functionally interacting at the plasma membrane with several protein partners, Cav3 influences an array of biological functions, thus configuring as a membrane sensor. Generation of Cav3 transgenic and knock-out animal models has clearly suggested that balanced levels of Cav3 are required to maintain the muscle homeostasis, as both its lack and excess compromise the integrity of skeletal muscle apparatus [12,15,21,22,43]. In addition, previous works have shown that loss of Cav3 inhibits myoblast differentiation [44,45] or causes death of cultured muscle cells [46]. In the present study we provide evidence that both lack and over-expression of Cav3 affect the *in vitro* process of myoblast fusion, thus confirming previous *in vivo* findings. Nevertheless, loss of Cav3 induced by Cav3 (P104L) form, but not the overexpression, elicited an immature cell and molecular signature due to the simultaneous attenuation of both Akt and p38 MAPK pathways, the main signalling networks by which the autocrine/paracrine extracellular cues signal into myoblasts to drive to the fusion process [29, 47-50]. In support of this evidence, a previous work showed that a down-regulation of both Akt and p38 pathways occurs in Cav3 null myoblasts, leading to reduced

insulin-stimulated glucose uptake [14]. Interestingly, Cav3 synthesis increases during differentiation of muscle cells quite dependently on the activation of both Akt and p38 pathways [44,45], suggesting that its localization at the plasma membrane might further provide a positive loop for the regulation of this signalling network. In this perspective, Cav3 configures as a key player of the myoblast fusion, and, accordingly, it has been recently shown that disruption of focal adhesion kinase signaling impairs myoblast fusion leading to selective down-regulation of Cav3 [51]. While a close link between Cav3 and Akt kinase activity has been already demonstrated [13-15], the potential relationship with p38 should be taken into account, being the activation of this pathway pivotally involved in the process of myoblast fusion upon N-cadherin ligation and the subsequent recruitment of the multifunctional cell surface Cdo protein [52,53]. Another point of interest in this work concerned the investigation of TGF-β signalling, being this pathway involved in the muscular atrophy of transgenic Cav3 (P104L) mice [12]. Our results suggest that, in cultured myotubes, loss of Cav3 was *per se* not sufficient to perturb TGF-β pathways, indicating that the attenuation of Akt and p38 pathways occurred independently on TGF-β signalling to promote the failure of myogenic program. Interestingly, Cav3 (P104L) myotubes treated with TGF-β displayed the over-activation of Smad2 pathway together with a down-modulation of Erk1/2 pathway, suggesting that the combination of these events, rather than the sole over-activation of Smad2 [12], might contribute to affect the integrity of myofibers. Remarkably, the differentiation of Cav3 (P104L) myotubes was improved by treatment with IGF-1 or TSA [23,24] as effect of Akt and p38 reactivation and apparently regardless of the lack of Cav3 recovery at the plasma membrane. These results indicate that if Cav3 is not strictly essential for the Akt and p38 signalling, it might rather serve to facilitate or change the outcome of its activation, thus working as a sensor. These data also suggest that the contribute of molecules sustaining Akt and p38 activities might partially counter the damages in Cav3-deficient muscles. Finally, another interesting feature which should be taken in account concerns the ability of a mutated Caveolin-1 (P132L) form, the mutation ortholog to Cav3 (P104L), to confer an immature signature to human breast cancerous cells, leading to increased

invasiveness and metastatic potential [54]. In keeping with these findings, we hypothesize that the Cav3 (P104L) form might behave with a similar fashion in skeletal muscle, imposing an immature cell and molecular signature by limiting the activity of Akt and p38 signalling network.

References

[1] R.G. Parton, K. Simons, The multiple faces of caveolae, Nat. Rev. Mol. Cell Biol. 8 (2007) 185–194.

[2] H.H. Patel, F. Murray, P.A. Insel, Caveolae as organizers of pharmacologically relevant signal transduction molecules, Annu. Rev. Pharmacol. Toxicol. 48 (2008) 359-91.

[3] T.M. Williams, M.P. Lisanti, The Caveolin genes: From cell biology to medicine, Annals of Medicine, 36 (2004) 584–895.

[4] M. Way, R.G. Parton, M-caveolin, a muscle-specific caveolin-related protein, FEBS Lett. 378 (1996) 108-12.

[5] Z. Tang, P.E. Scherer, T. Okamoto, K. Song, C. Chu, D.S. Kohtz, I. Nishimoto, H.F. Lodish, M.P. Lisanti, Molecular cloning of caveolin-3, a novel member of the caveolin gene family expressed predominantly in muscle, J Biol Chem. 271 (1996) 2255-61.

[6] R. Hnasko, M.P. Lisanti, The biology of caveolae: lessons from caveolin knockout mice and implications for human disease, Mol. Interv. 3 (2003) 445–464.

[7] V.J. Venema, H. Ju, R. Zou, R.C. Venema, Interaction of neuronal nitric-oxide synthase with caveolin-3 in skeletal muscle. Identification of a novel caveolin scaffolding/inhibitory domain, J Biol Chem. 272 (1997) 28187-90.

[8] G. García-Cardeña, P. Martasek, B.S. Masters, P.M. Skidd, J. Couet, S. Li, M.P. Lisanti, W.C. Sessa, Dissecting the interaction between nitric oxide synthase (NOS) and caveolin. Functional significance of the nos caveolin binding domain in vivo, J Biol Chem. 272 (1997) 25437-40.

[9] Y. Sunada, H. Ohi, A. Hase, H. Ohi, T. Hosono, S. Arata, S. Higuchi, K. Matsumura, T. Shimizu, Transgenic mice expressing mutant caveolin-3 show severe myopathy associated with increased nNOS activity, Hum Mol Genet. 10 (2001) 173-8.

[10] S. Li, J. Couet, M.P. Lisanti, Src tyrosine kinases, Ga subunits, and H-Ras share a common membrane-anchored scaffolding protein, caveolin. Caveolin binding negatively regulates the auto-activation of Src tyrosine kinases, J. Biol. Chem. 271 (1996) 29182-29190.

[11] G.M. Smythe, J.C. Eby, M.H. Disatnik, T.A. Rando, A caveolin-3 mutant that causes limb girdle muscular dystrophy type 1C disrupts Src localization and activity and induces apoptosis in skeletal myotubes, J Cell Sci. 116 (2003) 4739 –49.

[12] Y. Ohsawa, H. Hagiwara, M. Nakatani, A. Yasue, K. Moriyama, T. Murakami, K. Tsuchida, S. Noji, Y. Sunada, Muscular atrophy of caveolin-3-deficient mice is rescued by myostatin inhibition, J Clin Invest. 116 (2006) 2924-34.

[13] J. Oshikawa, K. Otsu, Y. Toya, T. Tsunematsu, R. Hankins, J. Kawabe, S. Minamisawa, S. Umemura, Y. Hagiwara, Y. Ishikawa, Insulin resistance in skeletal muscles of caveolin-3-null mice, Proc Natl Acad Sci U S A. 101 (2004) 12670-5.

[14] K. Fecchi, D. Volonte, M.P. Hezel, K. Schmeck, F. Galbiati, Spatial and temporal regulation of GLUT4 translocation by flotillin-1 and caveolin-3 in skeletal muscle cells, FASEB J. 20 (2006) 705-7.

[15] F. Capozza, T.P. Combs, A.W. Cohen, Y.R. Cho, S.Y. Park, W. Schubert, T.M. Williams, D.L. Brasaemle, L.A. Jelicks, P.E. Scherer, J.K. Kim, M.P. Lisanti, Caveolin-3 knockout mice show increased adiposity and whole body insulin resistance, with ligand-induced insulin receptor instability in skeletal muscle, Am J Physiol Cell Physiol. 288 (2005) C1317-31.

[16] C. Minetti, F. Sotgia, C. Bruno, P. Scartezzini, P. Broda, M. Bado, E. Masetti, P. Mazzocco, A. Egeo, M.A. Donati, D. Volonté, F. Galbiati, G. Cordone, F.D. Bricarelli, M.P.

Lisanti, F. Zara, Mutations in the caveolin-3 gene cause autosomal dominant limb-girdle muscular dystrophy, Nat. Genet. 18 (1998) 365-368.

[17] S.E. Woodman, F. Sotgia, F. Galbiati, C. Minetti, M.P. Lisanti, Caveolinopathies: mutations in caveolin-3 cause four distinct autosomal dominant muscle diseases, Neurology 62 (2004) 538-43.

[18] E. Gazzerro, F. Sotgia, C. Bruno, M.P. Lisanti, C. Minetti, Caveolinopathies: from the biology of caveolin-3 to human diseases, Eur J Hum Genet. 18 (2010) 137-45.

[19] F. Galbiati, D. Volonte, C. Minetti, J.B. Chu, M.P. Lisanti, Phenotypic behavior of caveolin-3 mutations that cause autosomal dominant limb girdle muscular dystrophy (LGMD-1C). Retention of LGMD-1C caveolin-3 mutants within the golgi complex, J Biol Chem. 274 (1999) 25632-41.

[20] F. Galbiati, D. Volonte, C. Minetti, D.B. Bregman, M.P. Lisanti, Limb-girdle muscular dystrophy (LGMD-1C) mutants of caveolin-3 undergo ubiquitination and proteasomal degradation, J Biol Chem. 275 (2000) 37702-11.

[21] S.J. Nixon, J. Wegner, C. Ferguson, P.F. Mery, J.F. Hancock, P.D. Currie, B. Key, M. Westerfield, R.G. Parton, Zebrafish as a model for caveolin-associated muscle disease; caveolin-3 is required for myofibril organization and muscle cell patterning, Hum Mol Genet. 14 (2005) 1727-43.

[22] F. Galbiati, D. Volonte, J.B. Chu, M. Li, S.W. Fine, M. Fu, J. Bermudez, M. Pedemonte, K.M. Weidenheim, R.G. Pestell, C. Minetti, M.P. Lisanti, Transgenic overexpression of caveolin-3 in skeletal muscle fibers induces a Duchenne-like muscular dystrophy phenotype, Proc Natl Acad Sci U S A. 97 (2000) 9689-94.

[23] A. Musarò, N. Rosenthal, Maturation of the myogenic program is induced by postmitotic expression of insulin-like growth factor I, Mol Cell Biol. 19 (1999) 3115-24.

[24] S. Iezzi, M. Di Padova, C. Serra, G. Caretti, C. Simone, E. Maklan, G. Minetti, P. Zhao, E.P. Hoffman, P.L. Puri, V. Sartorelli, Deacetylase inhibitors increase muscle cell size by

promoting myoblast recruitment and fusion through induction of follistatin, Dev Cell. 6 (2004) 673-84.

[25] N. Rosenthal, J.M. Kornhauser, M. Donoghue, K.M. Rosen, J.P. Merlie, Myosin light chain enhancer activates muscle-specific, developmentally regulated gene expression in transgenic mice, Proc Natl Acad Sci U S A. 86 (1989) 7780-4.

[26] P.L. Puri, M.L. Avantaggiati, C. Balsano, N. Sang, A. Graessmann, A. Giordano, M. Levrero, p300 is required for MyoD-dependent cell cycle arrest and muscle-specific gene transcription, EMBO J. 16 (1997) 369–383.

[27] V. Sartorelli, J. Huang, Y. Hamamori, L. Kedes, Molecular mechanisms of myogenic coactivation by p300: direct interaction with the activation domain of MyoD and with the MADS box of MEF2C, Mol. Cell. Biol. 17 (1997) 1010–1026.

[28] N. Nakamura, C. Rabouille, R. Watson, T. Nilsson, N. Hui, P. Slusarewicz, T.E. Kreis, G. Warren, Characterization of a cis-Golgi matrix protein, GM130, J Cell Biol. 131 (1995) 1715-26.

[29] Y. Li, B. Jiang, W.Y. Ensign, P.K. Vogt, J. Han, Myogenic differentiation requires signalling through both phosphatidylinositol 3-kinase and p38 MAP kinase, Cell Signal. 12 (2000) 751-57.

[30] C.A. Berkes, S.J. Tapscott, MyoD and the transcriptional control of myogenesis, Semin Cell Dev Biol. 16 (2005) 585-95.

[31] F. Le Grand, M.A. Rudnicki, Skeletal muscle satellite cells and adult myogenesis, Curr Opin Cell Biol. 19 (2007) 628-33.

[32] Z. Yablonka-Reuveni, M.A. Rudnicki, A.J. Rivera, M. Primig, J.E. Anderson, P. Natanson, The transition from proliferation to differentiation is delayed in satellite cells from mice lacking MyoD, Dev Biol. 210 (1999) 440-55.

[33] J.M. Dahlman, J. Wang, N. Bakkar, D.C. Guttridge, The RelA/p65 subunit of NF-kappaB specifically regulates cyclin D1 protein stability: implications for cell cycle withdrawal and skeletal myogenesis, J Cell Biochem. 106 (2009) 42-51.

[34] W. Yang, Y. Zhang, Y. Li, Z. Wu, D. Zhu, Myostatin induces cyclin D1 degradation to cause cell cycle arrest through a phosphatidylinositol 3-kinase/AKT/GSK-3 beta pathway and is antagonized by insulin-like growth factor 1, J Biol Chem. 282 (2007) 3799-808.

[35] M. Ji, Q. Zhang, J. Ye, X. Wang, W. Yang, D. Zhu, Myostatin induces p300 degradation to silence cyclin D1 expression through the PI3K/PTEN/Akt pathway, Cell Signal. 20 (2008) 1452-8.

[36] E. Perdiguero, V. Ruiz-Bonilla, L. Gresh, L. Hui, E. Ballestar, P. Sousa-Victor, B. Baeza-Raja, M. Jardí, A. Bosch-Comas, M. Esteller, C. Caelles, A.L. Serrano, E.F. Wagner, P. Muñoz-Cánoves, Genetic analysis of p38 MAP kinases in myogenesis: fundamental role of p38alpha in abrogating myoblast proliferation, EMBO J. 26 (2007) 1245-56.

[37] R. Derynck, Y.E. Zhang, Smad-dependent and Smad-independent pathways in TGF-beta family signalling, Nature 425 (2003) 577-84.

[38] J. Massaguè, R.R. Gomis, The logic of TGFbeta signaling, FEBS Lett. 580 (2006) 2811-20.

[39] A.U. Trendelenburg, A. Meyer, D. Rohner, J. Boyle, S. Hatakeyama, D.J. Glass, Myostatin reduces Akt/TORC1/p70S6K signaling, inhibiting myoblast differentiation and myotube size, Am J Physiol Cell Physiol. 296 (2009) C1258-70.

[40] M.R. Morissette, S.A. Cook, C. Buranasombati, M.A. Rosenberg, A. Rosenzweig, Myostatin inhibits IGF-I-induced myotube hypertrophy through Akt, Am J Physiol Cell Physiol. 297 (2009) C1124-32.

[41] B. Langley, M. Thomas, A. Bishop, M. Sharma, S. Gilmour, R. Kambadur, Myostatin inhibits myoblast differentiation by down-regulating MyoD expression, J Biol Chem. 277 (2002) 49831-40.

[42] D. Joulia, H. Bernardi, V. Garandel, F. Rabenoelina, B. Vernus, G. Cabello, Mechanisms involved in the inhibition of myoblast proliferation and differentiation by myostatin, Exp Cell Res. 286 (2003) 263-75.

[43] F. Galbiati, J.A. Engelman, D. Volonte, X.L. Zhang, C. Minetti, M. Li, H.J. Hou, B. Kneitz, W. Edelmann, M.P. Lisanti, Caveolin-3 null mice show a loss of caveolae, changes in the microdomain distribution of the dystrophin-glycoprotein complex, and t-tubule abnormalities, J Biol Chem. 276 (2001) 21425-33.

[44] F. Galbiati, D. Volonte, JA. Engelman, P.E. Scherer, M.P. Lisanti, Targeted down-regulation of caveolin-3 is sufficient to inhibit myotube formation in differentiating C2C12 myoblasts. Transient activation of p38 mitogen-activated protein kinase is required for induction of caveolin-3 expression and subsequent myotube formation, J Biol Chem. 274 (1999) 30315-21.

[45] A. Fanzani, E. Stoppani, L. Gualandi, R. Giuliani, F. Galbiati, S. Rossi, A. Fra, A. Preti, S. Marchesini, Phenotypic behavior of C2C12 myoblasts upon expression of the dystrophy-related caveolin-3 P104L and TFT mutants. FEBS Lett. 581 (2007) 5099-104.

[46] G.M. Smythe, T.A. Rando, Altered caveolin-3 expression disrupts PI(3) kinase signaling leading to death of cultured muscle cells, Exp Cell Res. 312 (2006) 2816-25.

[47] C. Rommel, S.C. Bodine, B.A. Clarke, R. Rossman, L. Nunez, T.N. Stitt, G.D. Yancopoulos, D.J. Glass, Mediation of IGF-1-induced skeletal myotube hypertrophy by PI(3)K/Akt/mTOR and PI(3)K/Akt/GSK3 pathways, Nat Cell Biol. 11 (2001) 1009-13.

[48] A. Zetser, E. Gredinger, E. Bengal, p38 mitogen-activated protein kinase pathway promotes skeletal muscle differentiation. Participation of the Mef2c transcription factor, J Biol Chem. 274 (1999) 5193-200.

[49] Z. Wu, P.J. Woodring, K.S. Bhakta, K. Tamura, F. Wen, J.R. Feramisco, M. Karin, J.Y. Wang, P.L. Puri, p38 and extracellular signal-regulated kinases regulate the myogenic program at multiple steps, Mol Cell Biol. 20 (2000) 3951-64.

[50] C. Serra, D. Palacios, C. Mozzetta, S.V. Forcales, I. Morantte, M. Ripani, D.R. Jones, K. Du, U.S. Jhala, C. Simone, P.L. Puri, Functional interdependence at the chromatin level between the MKK6/p38 and IGF1/PI3K/AKT pathways during muscle differentiation, Mol Cell. 28 (2007) 200-13.

[51] N.L. Quach, S. Biressi, L.F. Reichardt, C. Keller, T.A., Rando, Focal adhesion kinase signaling regulates the expression of caveolin 3 and beta1 integrin, genes essential for normal myoblast fusion, Mol Biol Cell. 20 (2009) 3422-35.

[52] G. Takaesu, J.S. Kang, G.U. Bae, M.J. Yi, C.M. Lee, E.P. Reddy, R.S. Krauss, Activation of p38alpha/beta MAPK in myogenesis via binding of the scaffold protein JLP to the cell surface protein Cdo, J Cell Biol. 175 (2006) 383-8.

[53] M. Lu, R.S. Krauss, N-cadherin ligation, but not Sonic hedgehog binding, initiates Cdo-dependent p38alpha/beta MAPK signaling in skeletal myoblasts, Proc Natl Acad Sci U S A. 107 (2010) 4212-7.

[54] G. Bonuccelli, M.C. Casimiro, F. Sotgia, C. Wang, M. Liu, S. Katiyar, J. Zhou, E. Dew, F. Capozza, K.M. Daumer, C. Minetti, J.N. Milliman, F. Alpy, M.C. Rio, C. Tomasetto, I. Mercier, N. Flomenberg, P.G. Frank, R.G. Pestell, M.P. Lisanti, Caveolin-1 (P132L), a common breast cancer mutation, confers mammary cell invasiveness and defines a novel stem cell/metastasis-associated gene signature, Am J Pathol. 174 (2009) 1650-62.

Acknowledgements

We thank Pier Lorenzo Puri (Telethon Dulbecco Institute, Rome, Italy) for providing the MCK and 4RE reporter vectors. This work was supported by Associazione Amici per il Cuore-ONLUS, Chiari (BS)-Italy to A.F. and E.M., by Fondazione Cariplo grant to E.M. and by University of Brescia research fund (ex 60%) to A.F.

Figure legends

Figure 1

Myoblast fusion is more severely affected by loss rather than excess of Cav3 at the plasma membrane.

C2C12 myoblasts were stably transfected with an empty vector (control) or vectors harbouring either Cav3 (P104L) or wild-type Cav3 (wtCav3) forms. A, after two days of differentiation, PCR and Western-Blot (WB) analyses detected Cav3 transcript and protein in transfected myoblasts. Under the same conditions, protein content of MyHC was evaluated. B, confocal microscopic images showing that Cav3 was mislocalized to perinuclear Golgi regions in Cav3 (P104L) myoblasts, as indicated by the merged staining with GM130 marker. In contrast, wtCav3 over-expression produced a labelling predominantly localized at the plasma membrane, as observed in control. Bars = 100 μm. Graphical panel reporting the average number of myotubes observed after differentiation of control and transfected myoblasts for up to day 2. Myotubes containing two or more nuclei were counted in ten different microscopic fields. Data are representative of two independent experiments.

Figure 2

Cav3 (P104L) expression impairs the differentiation of C2C12 and L6E9 myoblasts.

Control and C2C12 and L6E9 myoblasts, stably transfected with MLC- or CMV-Cav3 (P104L) vectors, were cultured in DM for up to day 4. A, immunofluorescent staining (IF) showing that Cav3 properly localized at the plasma membrane in control C2C12 myotubes, whereas in transfected cells accumulated in perinuclear regions without reaching the plasma membrane, as indicated by the arrows. Under these conditions, differentiation of MLC- or CMV-Cav3 (P104L) myoblasts was morphologically impaired compared to control (Giemsa staining, phase contrast pictures). Bars = 100 μm. B, the graphs report the average number of myotubes observed in control and Cav3 (P104L) myoblasts. Results are representative of three independent experiments. Significant at $p<0.05$ (*) or 0.01 (**) vs. control. C, Western-blot analyses of myogenin and MyHC,

as detected in control and Cav3 (P104L) myoblasts over a time-course differentiation. Tubulin was used as loading control.

Figure 3

Loss of Cav3, induced by Cav3 (P104L) expression, decreases the activity of Akt and p38 signalling, conferring an immature cell and molecular signature.

A, Western-blot analyses of Akt and p38 forms (phosphorylated vs. total), as detected in control and MLC-Cav3 (P104L) myoblasts over a time-course differentiation. Under the same conditions, the expression of different protein markers was analyzed. Tubulin was used as loading control. B, graphical representation of MyoD, Myf-5 and myogenin transcript levels, obtained by RT-PCR analysis, as detected in control and MLC-Cav3 (P104L) myoblasts over a time-course differentiation. GAPDH was used to normalize expression. Results are representative of three independent experiments. Significant at $p<0.05$ (*) vs. control. C, luciferase reporter assays were performed to evaluate the ability of MyoD to transactivate two different MyoD-responsive promoters, consisting of a MCK promoter or a minimal 4RE element, which were transiently transfected in control C2C12 and MLC-Cav3 (P104L) myoblasts for up to 24 hours in DM. The reporter expression was expressed as the ratio between the activity from Firefly and Renilla luciferase. Results are representative of three independent experiments. Significant at $p<0.01$ (**) vs. control. D, Western-blot analyses of Akt and p38 forms (phosphorylated vs. total), as detected in control and wtCav3-overexpressing myoblasts after 24 hours of differentiation. Tubulin was used as loading control.

Figure 4

In C2C12 myoblasts the pharmacological inhibition of both Akt and p38 pathways triggers the molecular signature observed in Cav3 (P104L) myoblasts.

A, Western-blot analyses of MyoD, Myf-5 and cyclin D1, as detected in C2C12 cells cultured in DM and left untreated (DMSO) or treated with SB or LY for up to day 2. Tubulin was used as loading control. B, phase contrast pictures showing morphology of C2C12 myoblasts cultured in

DM in presence of DMSO (vehicle) or both 5 μM SB and LY for up to day 2. Bars = 100 μm. C, Western-blot analyses of MyoD, Myf-5, cyclin D1 and myogenin, as detected in C2C12 cells cultured in DM in presence of DMSO or both SB and LY inhibitors. Tubulin was used as loading control. D, in C2C12 cells transiently transfected with a minimal 4-RE element for up to 24 hours, the ability of MyoD to transactivate the luciferase reporter was prevented in presence of both SB and LY treatment compared to DMSO. Results are representative of three independent experiments. Significant at $p<0.05$ (*) vs. DMSO.

Figure 5

Lack of Cav3 perturbs the activation of TGF-β pathways.

Western-blot analyses of Smad2, Smad3 and Erk1/2 phosphorylation, as detected in control C2C12 and MLC- or CMV-Cav3 (P104L) myoblasts differentiated for up to day 2, and then left untreated or treated with 5 ng/ml TGF-β for the indicated time-points. Tubulin was used as loading control. Relative quantifications are graphically shown. Results are representative of three independent experiments. Significant at $p<0.05$ (*) vs. control.

Figure 6

IGF-1 or TSA treatments significantly improve the differentiation of MLC-Cav3 (P104L) myoblasts.

Control and MLC-Cav3 (P104L) myoblasts were cultured in DM, exposed to TSA or treated with IGF-1 (as described in Materials and Methods). A, phase contrast pictures showing the morphology of control and MLC-Cav3 (P104L) myoblasts exposed to the different treatments for up to day 4. Under the same conditions, immunofluorescence (IF) was performed to stain MyHC and Cav3. Bars = 100 μm. B-C, the average number and area of control and MLC-Cav3 (P104L) myotubes have been quantified in the absence or presence of IGF-1 and TSA. Results are representative of three independent experiments. Significant at $p<0.05$ (*) vs. DM. D, upon TSA exposure followed by post-mitotic treatment with IGF-1, MLC-Cav3 (P104L) myotubes developed a giant size, despite being evident the perinuclear accumulation of Cav3. Bars = 100 μm.

Figure 7

IGF-1 or TSA treatments, by enabling Akt and p38 signalling, restore the expression of myogenic markers in Cav3 (P104L) myotubes.

A, follistatin levels were monitored by RT-PCR analysis in control and MLC-Cav3 (P104L) myoblasts, after treatment with DMSO or TSA and subsequent exposure to DM for up to 24 hours. GAPDH was used to normalize expression. B, Western-blot analyses of the Akt and p38 forms (phosphorylated vs. total), as detected in control and MLC-Cav3 (P104L) cells subjected to IGF-1 from day 2 to day 3, or exposed to TSA. Tubulin was used as loading control. C, Western-blot analyses of MyoD, Myf-5 and myogenin, as detected in control and MLC-Cav3 (P104L) myoblasts cultured in DM, exposed to TSA or post-mitotically treated with IGF-1 for the indicated time-points. Tubulin was used as loading control. Numbers below the panels indicate the protein quantification, calculated as the ratio between each band protein and the respective tubulin. D, upon the same treatments seen above, Western-blot analyses detected the levels of MyHC in control and MLC-Cav3 (P104L) myotubes after 4 days of differentiation.

Author's statement

The authors declare that the material includes an original research, which has not been previously published and has not been submitted for publication elsewhere while under consideration.

Conflict of interest.

The authors declare no conflict of interest.

Figure
Click here to download high resolution image

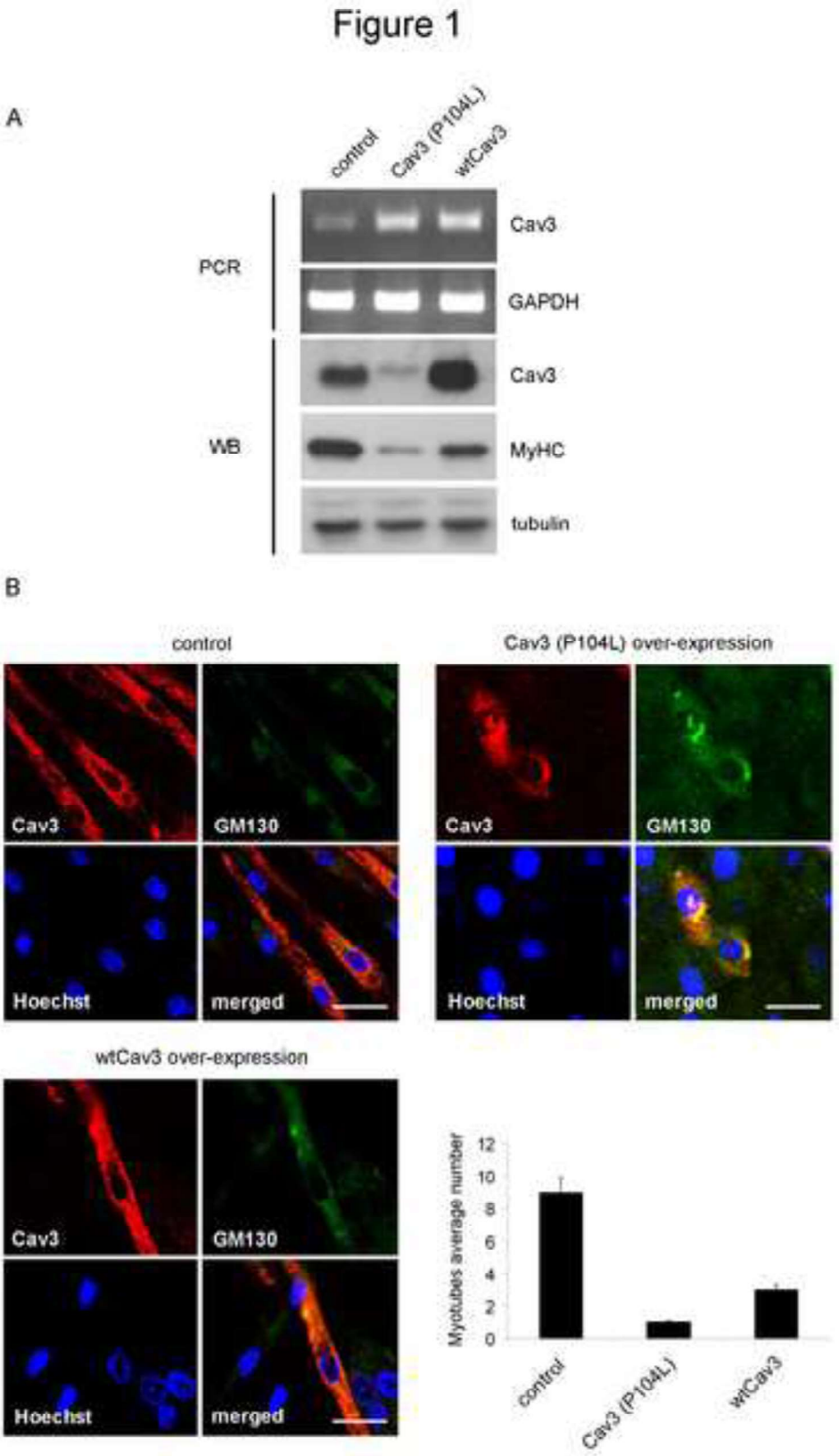

Figure
Click here to download high resolution image

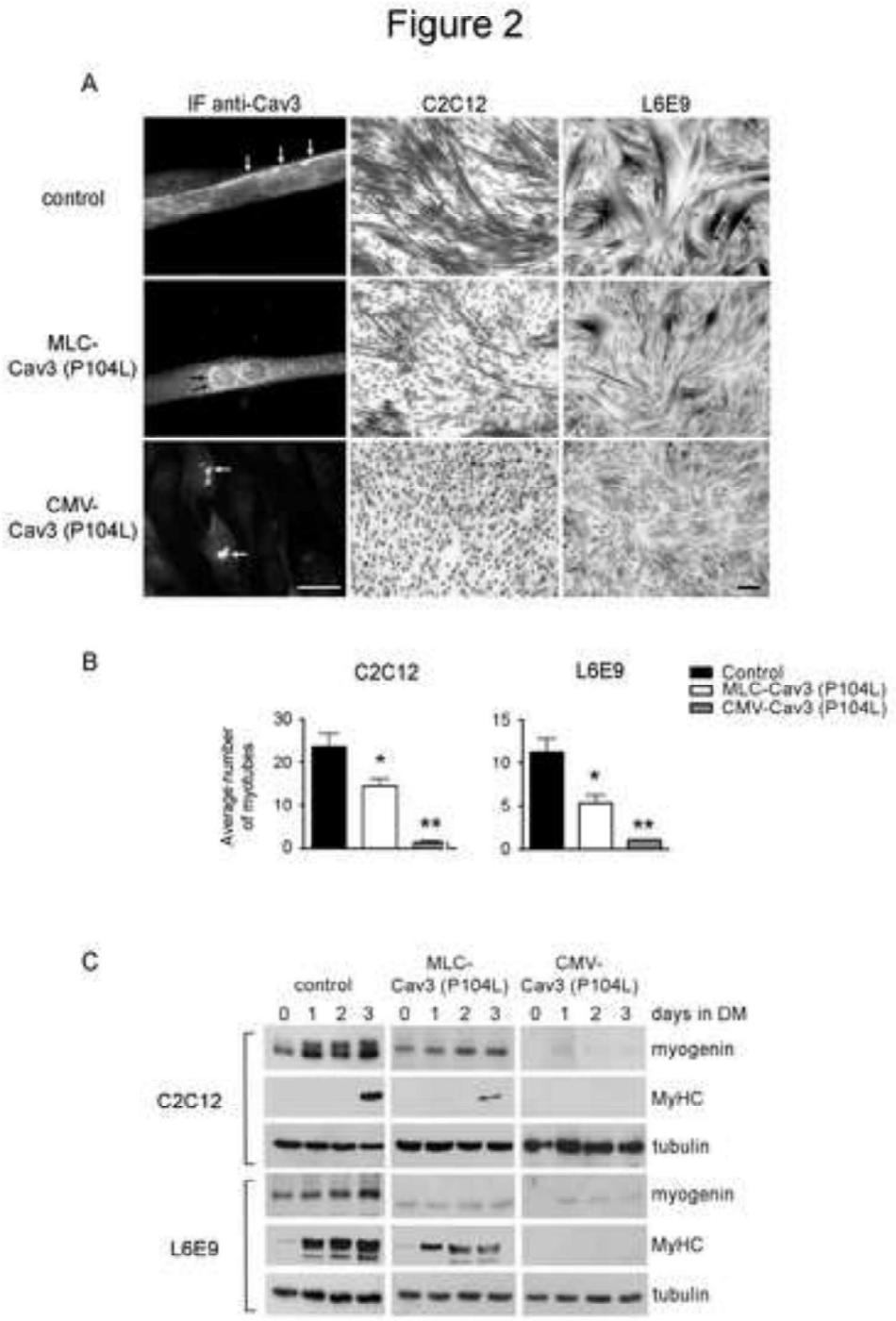

Figure
Click here to download high resolution image

Figure 3

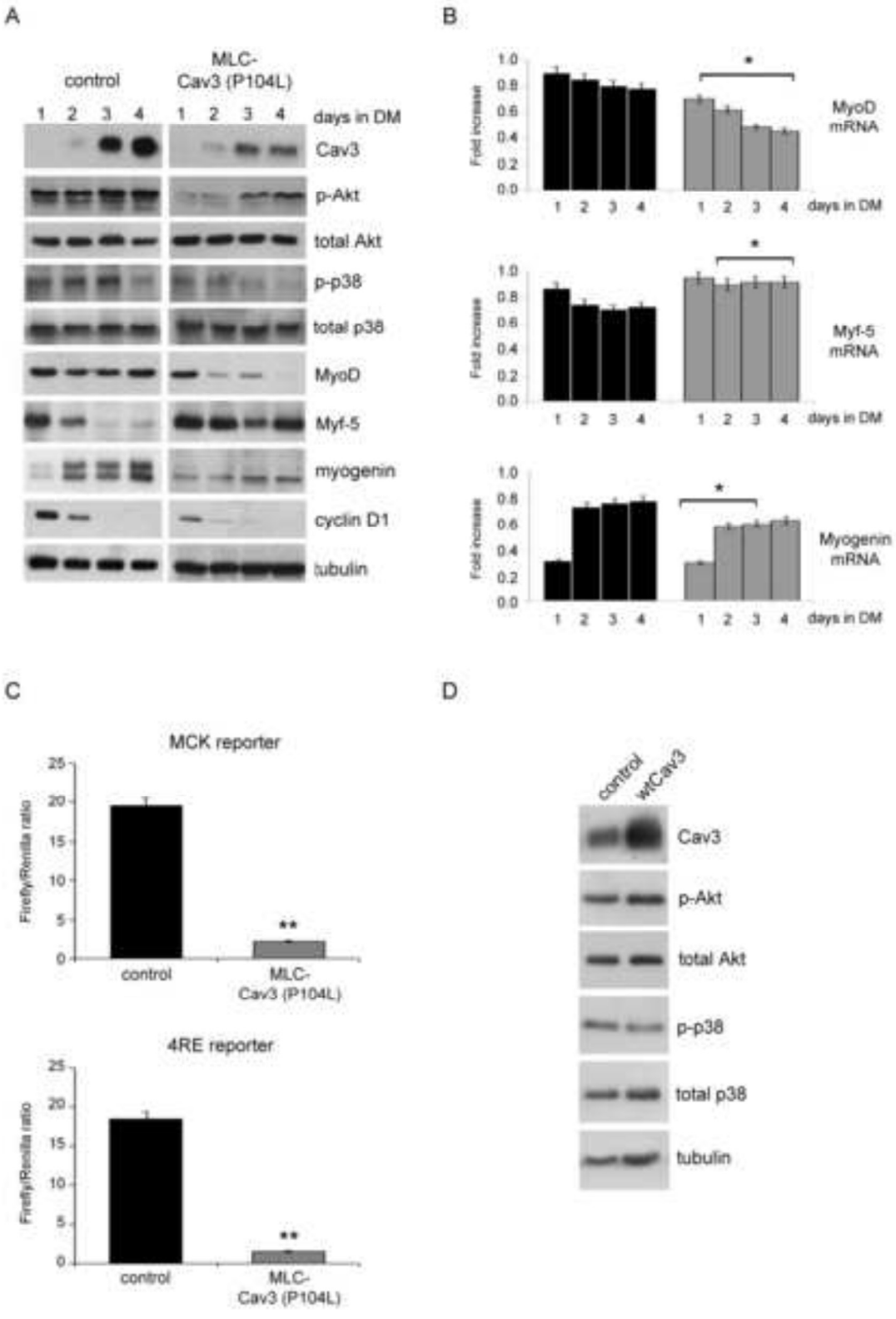

Figure
Click here to download high resolution image

Figure 4

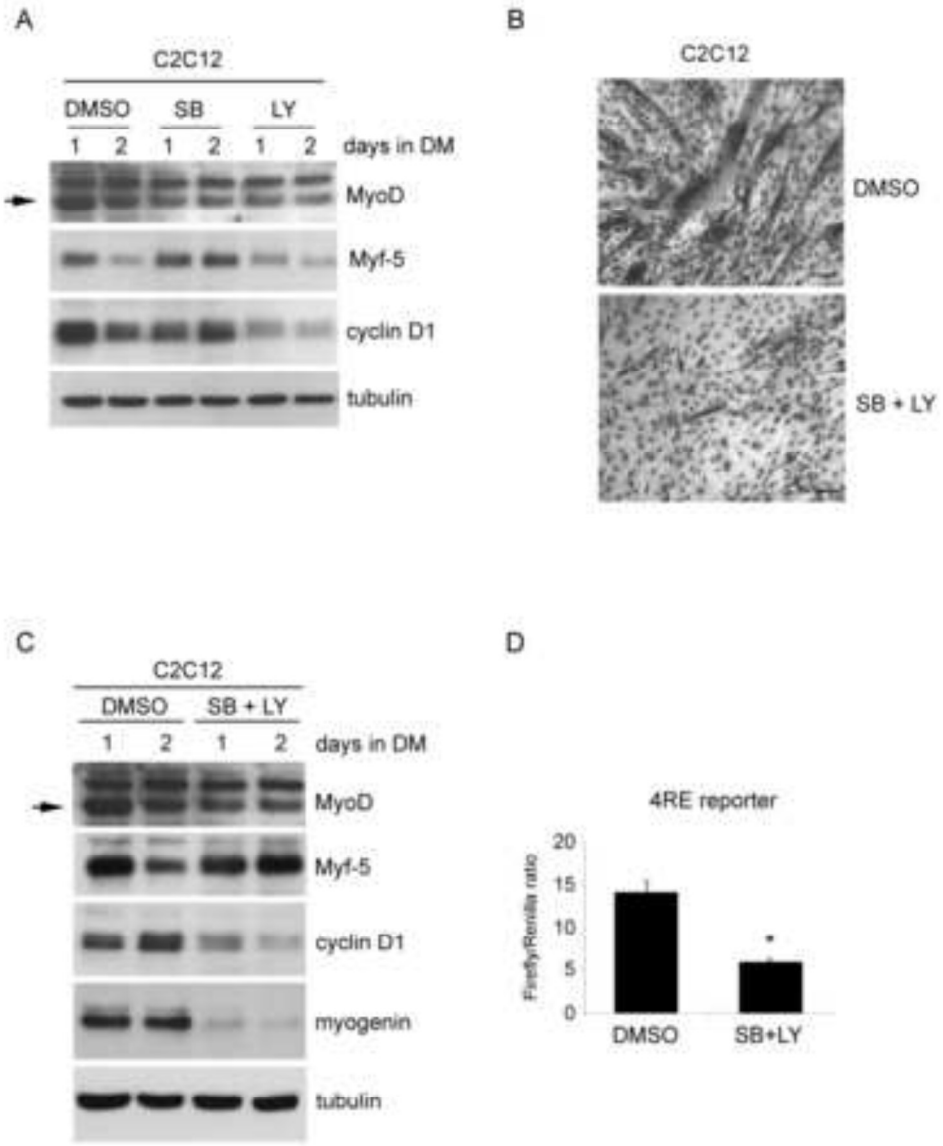

Figure
Click here to download high resolution image

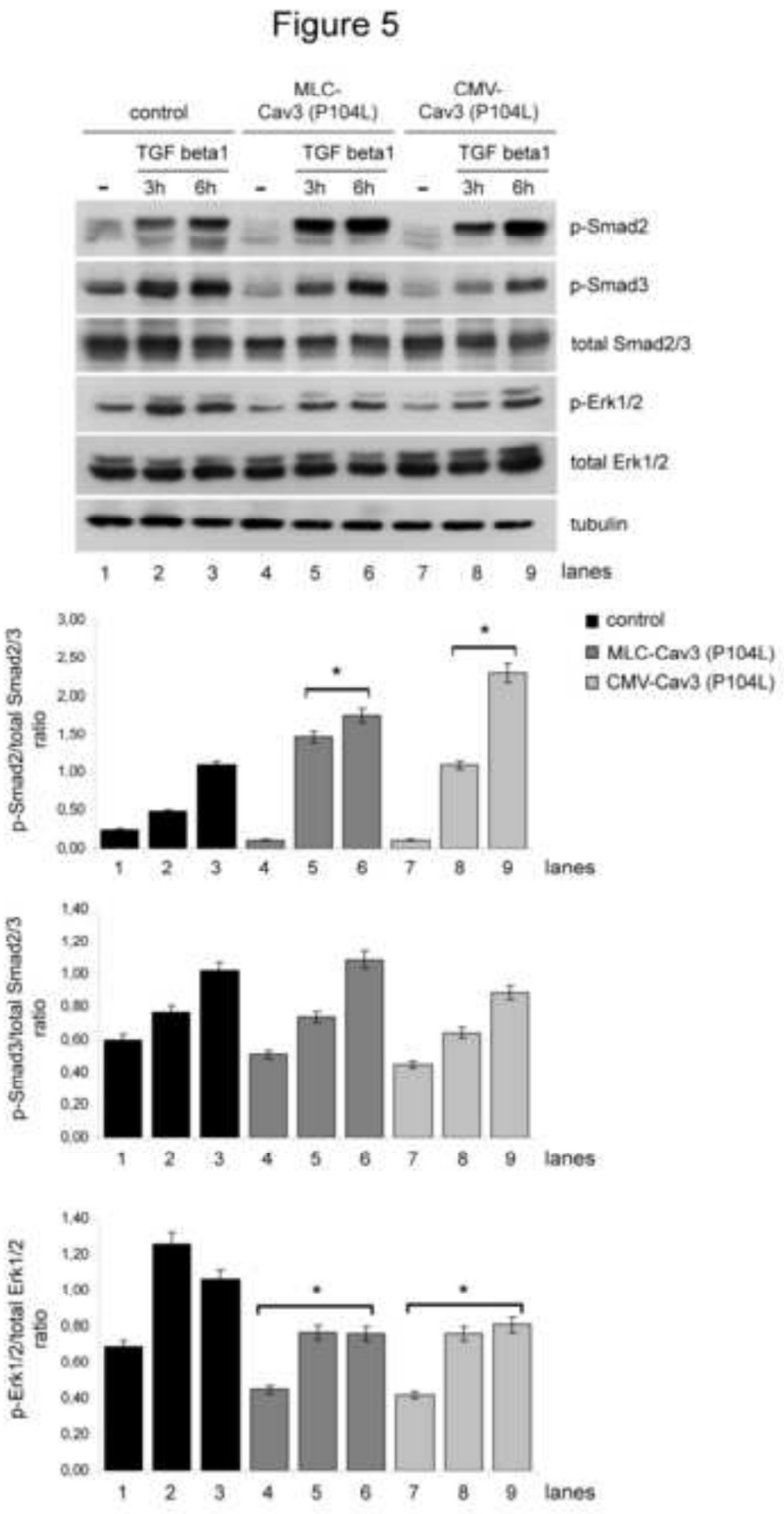

Figure
Click here to download high resolution image

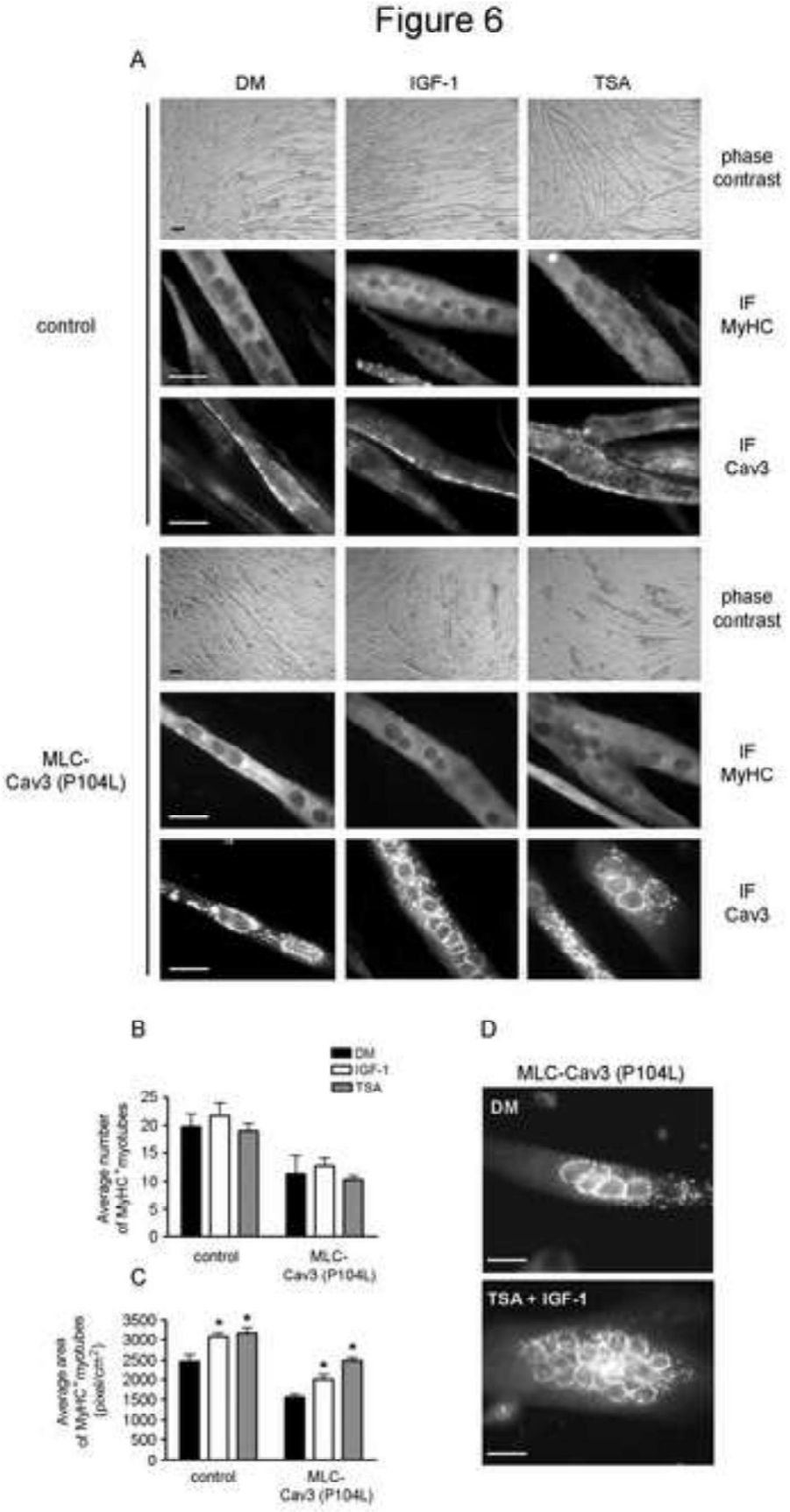

Figure
Click here to download high resolution image

Figure 7